

TOPOLOGY OPTIMIZATION INCLUDING INEQUALITY BUOYANCY CONSTRAINTS

R. PICELLI*, R. VAN DIJK[†], W.M. VICENTE*, R. PAVANELLO*, M.
LANGELAAR[‡] AND F. VAN KEULEN[‡]

*Faculty of Mechanical Engineering
University of Campinas
Rua Mendeleev 200, 13083-860, Campinas, Brazil
e-mail: picelli@fem.unicamp.br; web page: <http://www.unicamp.br>

[†]van Dijk FEM engineering B.V.
Simonsstraat 14, 2628 TH, Delft, The Netherlands
e-mail: ronald@vandijkfem.nl; web page: <http://www.vandijkfemengineering.nl>

[‡]Structural and Optimization Mechanics
Faculty of Mechanical, Maritime and Materials Engineering
Delft University of Technology
Mekelweg 2, 2628 CD, Delft, The Netherlands
e-mail: a.vankeulen@tudelft.nl; web page: 3me.tudelft.nl/som

Key words: Topology Optimization, BESO Method, Buoyancy, Buoyant Structures, Subsea Buoyancy Modules.

Abstract. This paper presents an evolutionary topology optimization method for applications in design of completely submerged buoyant devices with design-dependent fluid pressure loading. This type of structures aid rig installations and pipeline transportation in all water depths in offshore structural engineering. The proposed optimization method seeks the buoy design that presents higher stiffness, less material and a prescribed buoyancy effect. A hydrostatic fluid is used to simulate the underwater pressure and the polymer buoyancy module is considered linearly elastic. Both domains are solved with the finite element method. From the initial design domain, solid elements with low strain energy are iteratively removed until a certain prescribed volume fraction. The studied case consists in a buoy for supporting subsea oil pipelines, in which the inner diameter is constant and the outer shape and interior holes are defined by the optimization algorithm. A new buoyancy constraint is introduced in order to guarantee a satisfactory buoyancy effect.

1 INTRODUCTION

Since its introduction [1], topology optimization has reached a certain level of maturity enough to be applied in the industry, in the field of structural design. Through the last decade, the method has been under a considerable scientific effort in order to extend the idea to some other different problems, e.g. considering different objective functions and constraints or even multiphysics problems [2, 3]. Herein, the authors propose the use of topology optimization in the offshore structural engineering field, so far specifically in the design of completely submerged (subsea) buoyancy modules for oil pipelines support.

In order to design subsea polymer buoys, design-dependent underwater pressure loadings and buoyancy effects must be considered. Design-dependent pressure loads showed to be a challenging topic for topology optimization [4] and it is still an issue under research [5]. To the best of the authors' knowledge, buoyancy effects are considered for the first time in topology optimization in the presented paper. To deal with both pressure loads and buoyancy, an adapted fluid-structure Bi-directional Evolutionary Structural Optimization (BESO) method is proposed. The discrete nature of the evolutionary methods [6] allows the fluid-structure interfaces to be explicitly defined, which makes the pressure loads modeling straightforward. Buoyancy requirements are introduced as an inequality constraint in the optimization problem. The resulting buoyancy force is equivalent to the weight of the fluid displaced by the submerged structure, expressed as:

$$\mathbf{F}_B = -\rho_f V_f \mathbf{g}_a \tag{1}$$

where \mathbf{F}_B is the buoyancy force acting on the structure, ρ_f is the mass density of the fluid, V_f the volume of the displaced fluid and \mathbf{g}_a the vector of the gravitational acceleration, expressed in the Cartesian coordinate system (x, y) as:

$$\mathbf{g}_a = \left\{ \begin{array}{c} 0 \\ -g_a \end{array} \right\} \tag{2}$$

where g_a is the value of the gravitational acceleration. As seen in Fig. 1, the force \mathbf{F}_B is balanced by the weight \mathbf{W}_s of the structure, expressed as:

$$\mathbf{W}_s = m_s \mathbf{g}_a \tag{3}$$

where m_s is the mass of the structure.

Considering that the mass of the structure is a constraint in the proposed optimization method, \mathbf{W}_s is constant and the only variable in the force diagram is \mathbf{F}_B , which depends exclusively on V_f , since ρ_f and g_a are also constant. Thus, in order to guarantee some desired buoyancy effects, the entire structural volume (including interior voids) must be as big as possible. The final goal of the optimization problem is then to design a structure stiffest as possible, handling design-dependent underwater pressure loads and presenting high buoyancy effects (high displaced fluid volume).

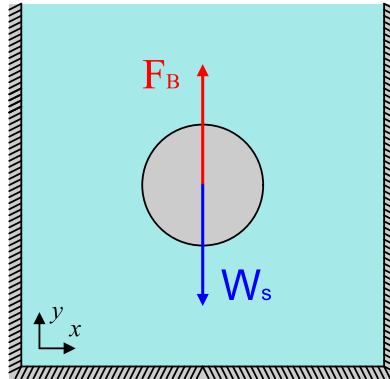


Figure 1: Force diagram with the resulting buoyancy force and weight acting on a completely submerged structure (gray sphere).

2 Methodology

2.1 Computational model

The topology optimization methods are based on the structural responses obtained computationally via the finite element method (FEM) [7]. With the FEM, the deformation of the structure under deep water pressure loadings can be simulated. The solid material is simulated with a static analysis using linearly elastic finite elements (without body forces), governed by the following equation:

$$\text{div}\sigma_s = \mathbf{0} \quad (4)$$

where σ_s is the Cauchy stress tensor. The pressure loading is simulated by simple fluid finite elements attached to the structural ones. The fluid is governed by the Laplace's equation

$$\nabla^2 P_f = 0 \quad (5)$$

where P_f is the pressure values throughout the fluid field. The final finite element model is

$$\begin{bmatrix} \mathbf{K}_s & -\mathbf{L}_{fs} \\ \mathbf{0} & \mathbf{K}_f \end{bmatrix} \begin{Bmatrix} \mathbf{u}_s \\ \mathbf{P}_f \end{Bmatrix} = \begin{Bmatrix} \mathbf{0} \\ \mathbf{0} \end{Bmatrix} \quad (6)$$

where \mathbf{K}_s and \mathbf{K}_f are the stiffness matrices of the structural and the fluid domains, respectively. The matrix \mathbf{L}_{fs} couples the fluid pressure with the structural analysis. Pressure values are imposed in some points of the pressure vector \mathbf{P}_f and, solving the previous system of equations, the structural displacements vector \mathbf{u}_s is obtained [7].

2.2 Optimization problem and sensitivity analysis

The evolutionary topology optimization problem for subsea buoyancy modules design can be stated as:

$$\begin{aligned}
& \text{Minimize} && f(x_i) = \frac{1}{2} \mathbf{u}_s^T \mathbf{K}_s \mathbf{u}_s + p \max(0, g) \\
& \text{Subject to:} && \begin{bmatrix} \mathbf{K}_s & -\mathbf{L}_{fs} \\ \mathbf{0} & \mathbf{K}_f \end{bmatrix} \begin{Bmatrix} \mathbf{u}_s \\ \mathbf{P}_f \end{Bmatrix} = \begin{Bmatrix} \mathbf{0} \\ \mathbf{0} \end{Bmatrix} \\
& && V_s - \sum_{i=1}^{nel} V_i x_i = 0 \\
& && x_i = [0, 1]
\end{aligned} \tag{7}$$

where

$$g = \frac{B_{lim}}{B} - 1 \leq 0 \tag{8}$$

$\frac{1}{2} \mathbf{u}_s^T \mathbf{K}_s \mathbf{u}_s$ is the structural mean compliance C , p is an arbitrary penalty factor, V_s is the prescribed final solid volume, nel is the number of elements inside the design domain and x_i represents the discrete design variables, in which 1 is a solid element and 0 is void. In this work, some void elements are substituted by fluid elements capable to transfer pressure values through the fluid domain. The term B_{lim} is the minimum required buoyancy area (displaced fluid area for 2D cases) and B is the buoyancy area of the current structural design. The inequality constraint g sets a threshold for the required buoyancy area and the equality constraint h sets the amount of solid material to be used with respect to the volume of the design domain. When B is lower than B_{lim} , g is higher than 0 and adds to the objective function $f(x_i)$. This behavior is then discouraged by a high penalty factor.

A sensitivity analysis is needed in order to determine the efficiency of each element in the structural performance and to decide which element should be eliminated or returned to solid condition. This analysis is carried out by deriving the objective function analytically with respect to the design variables. The derivatives of $f(x_i)$ with respect to x_i are:

$$\frac{\partial f(x_i)}{\partial x_i} = \alpha_C + p \alpha_B \tag{9}$$

where α_C and α_B correspond to the derivatives of the compliance and the buoyancy objectives, respectively. The derivatives of the mean compliance, including the design-dependent pressure loading term, can be expressed as:

$$\alpha_C = \frac{\partial C}{\partial x_i} = \mathbf{u}_s^T \frac{\partial \mathbf{L}_{fs}}{\partial x_i} \mathbf{P}_f - \frac{1}{2} \mathbf{u}_s^T \frac{\partial \mathbf{K}_s}{\partial x_i} \mathbf{u}_s \tag{10}$$

and the derivative on the buoyancy is

$$\alpha_B = \frac{\partial g}{\partial x_i} = \frac{\partial(\frac{B_{lim}}{B} - 1)}{\partial x_i} = B_{lim} \frac{\partial(\frac{1}{B})}{\partial x_i} = -B_{lim} \frac{1}{B^2} \frac{\partial B}{\partial x_i} \quad (11)$$

The analytical derivatives are then evaluated locally at the element level, which generates a sensitivity number for each element. Both compliance and buoyancy sensitivities must be normalized in order to be comparable between each other. Thus, the sensitivity numbers for buoyancy modules design using evolutionary methods can be expressed as:

$$\alpha_i = \frac{|\alpha_{C_i}|}{\max(|\alpha_{C_i}|)} + p \frac{|\alpha_{B_i}|}{\max(|\alpha_{B_i}|)} \quad (12)$$

where α_{C_i} and α_{B_i} are the sensitivities at the element level for both compliance and buoyancy objectives, respectively. The term α_{C_i} can be expressed as:

$$\alpha_{C_i} = \mathbf{u}_i^T \mathbf{L}_c^i \mathbf{P}_i - \frac{1}{2} \mathbf{u}_i^T \mathbf{K}_s^i \mathbf{u}_i \quad (13)$$

where \mathbf{u}_i and \mathbf{P}_i are the vectors with displacements and pressures at the i th element nodes, respectively. \mathbf{K}_s^i is the elemental stiffness matrix and \mathbf{L}_c^i is the change in the coupling configuration (see Fig. 3) due to the i th element removal (see Fig. 2). Only solid elements at the fluid-structure interfaces will have nonzero \mathbf{P}_i . For all the other elements the product $\mathbf{u}_i^T \mathbf{L}_c^i \mathbf{P}_i$ is zero.

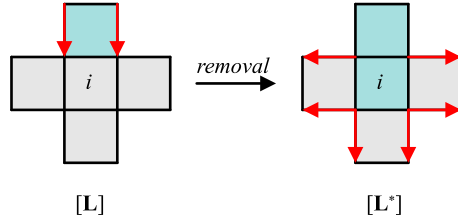


Figure 2: Coupling forces configuration before and after the i th element removal.

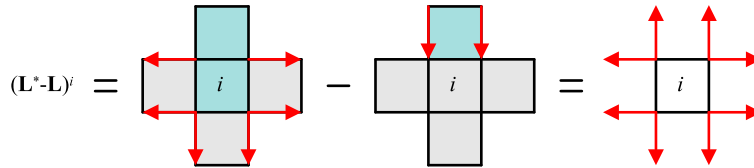


Figure 3: Change of the coupling matrices configuration $\frac{\partial \mathbf{L}_{fs}}{\partial x_i} \cong (\mathbf{L}^* - \mathbf{L})^i$ after the i th element removal.

The partial derivative $\frac{\partial B}{\partial x_i}$ from Eq. (11) can be evaluated at the element level as:

$$\left(\frac{\partial B}{\partial x_i}\right)^i \cong \Delta B(x_i) = (B^* - B)^i = (-A_i)^{fs} \quad (14)$$

where B^* is the buoyancy area after the i th element removal and the superscript fs indicates the term valid only for elements at the fluid-structural interfaces. Elements in the interior of the structure do not cause any change in B with their removal. Solid elements at the fluid-structural boundaries cause a change of $-A_i$, i.e., a decrease in B equivalent to the area A_i of the element. Then, the derivative corresponding to the buoyancy objective is a constant valid only for solid elements at the fluid-structural interface. For all the other elements, the sensitivity value is 0. Thus, recovering Eq. (11)

$$\alpha_{Bi} = \left(\frac{\partial g}{\partial x_i}\right)^i = \frac{B_{lim}}{B^2} (A_i)^{fs} \quad (15)$$

Recovering that α_i must be normalized, the second term of α_i is

$$p \frac{|\alpha_{Bi}|}{\max(|\alpha_{Bi}|)} = (p)^{fs} \quad (16)$$

The value of α_{Bi} is either a constant higher than zero or zero. This means that its maximum value is also α_{Bi} , which makes the result of the normalization as 1 for the solid elements at the fluid-structural boundaries and 0 for all the other elements.

Manipulating the first term of α_i and rewriting Eq. (12), the sensitivity numbers for buoyancy modules design are

$$\alpha_i = \begin{cases} \frac{1}{2} \mathbf{u}_i^T \mathbf{K}_s^i \mathbf{u}_i - \mathbf{u}_i^T \mathbf{L}_c^i \mathbf{P}_i + (p)^{fs} & x_i = 1 \\ 0 & x_i = 0 \end{cases} \quad (17)$$

It is important to point out that the term $(p)^{fs}$ is only valid when the inequality constraint g is violated. The first term of α_i is the strain energy of the element x_i . The second term is the derivative of the pressure loads at the element level. The elements with the lowest sensitivities can be removed from the domain with a minimum change in the objective function. When g is not violated, the compliance derivatives will provide the gradient information to the optimization procedure. For buoyant structures, the minimum compliance would be obtained with the smallest possible structure without holes, i.e., a structure with a very small B . However, while B is getting lower, g will be violated and the solid elements at the fluid-structure interfaces will have a high sensitivity number due to p . It will imply in the addition of elements beside the fluid-structure boundaries and in the expansion of the structure. Also at this step, only elements in the interior of the structure will be removed, which generates holes and makes the algorithm to obtain a higher B for a prescribed V_s .

A tolerance factor B_{tol} on the buoyancy area is also included. It allows B to be lower than B_{lim} when the structural volume V_n reaches V_s but the algorithm still did

not converged. For example, if the parameter B_{tol} is adopted as 80%, when $V_n = V_s$ the buoyancy area can be equal or greater than $0.8 \cdot B_{lim}$. Thus, the inequality constraint g becomes:

$$g = \frac{B_{tol} \cdot B_{lim}}{B} - 1 \leq 0 \quad (18)$$

This increases the solutions space and the buoyant structure can adjust itself in order to better support the pressure loadings, making the convergence easier.

2.3 The adapted fluid-structure BESO method

The evolutionary procedures of the presented BESO method for fluid pressure problems and buoyancy constraints are given as follows:

1. Discretize the design domain using a finite element (FE) mesh for the given boundary conditions. Initially, the global fluid-structure stiffness matrix must be assembled uncoupled.
2. Couple and store a current global matrix \mathbf{K}_n with the coupling matrices according to the current design of the n th iteration and appropriate boundary conditions. Thus, the current \mathbf{K}_n becomes equivalent to the stiffness matrix from the Eq. (6).
3. Perform FE analysis on the current design to obtain the fluid-structure responses.
4. Calculate the sensitivity numbers according to the Eq. (17).
5. Apply a mesh-independency filter scheme. Project the nodal sensitivity numbers to the design domain and smooth the sensitivity numbers for all (fluid and solid) elements in the design domain as described in [6].
6. Average the sensitivity numbers with their previous iteration ($n - 1$) numbers and then save the resulting sensitivity numbers for the next iteration.
7. Determine the target structural volume V_{n+1} for the next iteration as:

$$V_{n+1} = V_n(1 \pm ER) \quad (19)$$

where ER is the evolutionary ratio and n the number of the iteration. ER is the percentage of the initial design domain volume and increases or decreases V_{n+1} towards a structural desired final volume V_s . The target volume V_{n+1} sets the threshold α_{th} of the sensitivity numbers.

8. Construct a new fluid-structure design, by switching design variables x_i from 1 to 0 and from 0 to 1. Solid elements ($x_i = 1$) which

$$\alpha_i \leq \alpha_{th} \tag{20}$$

are switched to void (fluid) condition ($x_i = 0$). Void/fluid elements ($x_i = 0$) are switched to solid condition ($x_i = 1$) when

$$\alpha_i > \alpha_{th} \tag{21}$$

In order to control the fluid and void regions, a decision should be taken when the elements must have their design variables stated as $x_i = 0$. If the element has at least one fluid element as neighbor, it must be turned also into a fluid element. If the element does not have any fluid neighbors, the element must be turned into a void. This procedure can be repeated until there is no more changes in the fluid-void regions. Thus, fluid elements are kept together while the fluid region tracks the fluid-structure interface and void holes appear inside the structural domain.

9. Remove and/or add the elemental stiffness matrices from the original uncoupled global matrix according to the change of the current design.
10. Repeat steps 2-10 until the prescribed structural volume (V_s) is reached and a convergence criterion is satisfied. The mean compliance convergence is analyzed as:

$$error = \frac{|C_n - C_{n-1}| + |C_{n-1} - C_{n-2}|}{C_n - C_{n-1}} \leq \tau \tag{22}$$

where C is the mean compliance value and τ is the tolerance usually adopted as 0.001. When $error \leq \tau$, the algorithm stops.

3 Results

The study case is a subsea buoy design problem. The polymer buoy is built with two semicircles with inner and outer radius, in which the pipeline is attached to the buoy at the inner radius. This module is enclosed by a high pressure fluid domain in consequence by its deep water condition. Any other types of loads are considered negligible due to the high depth pressure case. For this buoyancy module problem, one of the semicircles is considered for design. The extended design domain is shown in Fig. 4. Figure 4(a) shows the structural floating model immersed on a pressurized fluid domain. The boundary conditions for the finite element model used is shown in Fig. 4(b), including symmetry condition and a blocked degree of freedom which makes the model non-singular. The inner edge (represented by a thick black line) is considered as non-design domain, i.e., it remains fixed during the whole algorithm.

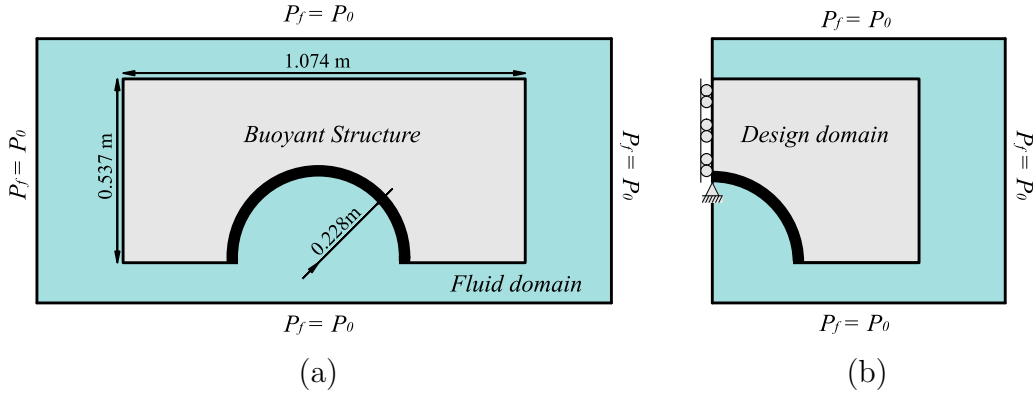


Figure 4: Design problem for optimization: (a) complete fluid-structure model and (b) design domain using half of the model including boundary conditions for the structure.

For the design problem from Fig. 4 two initial solutions are considered, one starting from the initial full design and another with an initial semicircle solution that covers 75% of the design domain. The fluid-structure model including the design domain is discretized with 51513 four-node finite elements. The evolutionary ratio (ER) is chosen to be 5% and the final volume V_s is adopted as 30%. Figure 5 presents the initial solutions and the final topologies for both cases, as well as a comparison case in which the fluid-structural interfaces are kept fixed. The buoyancy area limit B_{lim} is chosen as 0.1856 m^2 , which is the same area of the initial semicircle solution from Fig. 5(b-c). The penalty factor is chosen as $p = 1 \cdot 10^5$. The tolerance in buoyancy is adopted as $B_{tol} = 80\%$.

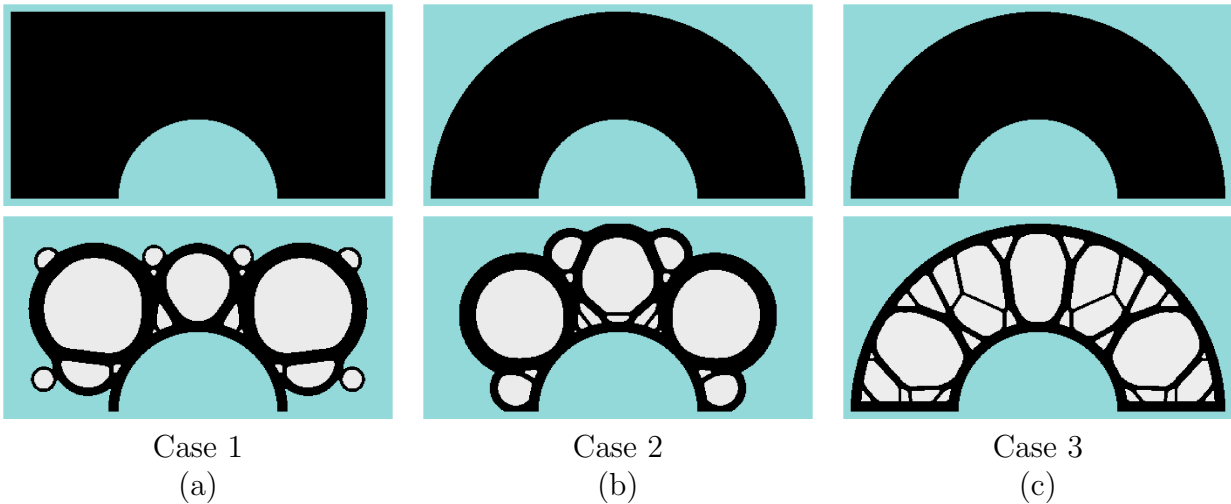


Figure 5: Buoy module designs with topology optimization: (a) Case 1: full design domain and final topology; (b) Case 2: initial semicircle solution and final topology; (c) Case 3: initial semicircle solution and final topology with fixed fluid-structure interfaces.

It is possible to observe that the final topologies (from Fig. 5(a) and 5(b)) mainly cover

the area of the initial guess solution. It characterizes a strong influence from the starting topology. Also, it indicates that the designer should choose the initial guess according to some desired final solution area. This behavior is expected due to the floating conditions. When pressure is applied all over a floating structure that can change its shape and topology, the structure starts seeking for an equilibrium state behaving like bubbles as found in the nature. The final results in this work are bubble-like structures.

Table 1 presents some objective data for all the cases from Fig. 5. Using the same amount of solid material, case 2 presents the stiffest structure. It represents a gain around 35% in stiffness if compared to the case 3, with a reduction in buoyancy area of only less than 16%. Case 1 did not show many gains in comparison with case 3. Also, it presented some very small bubble-like structures that contribute to local minima findings. Figures 6 e 7 presents the evolutionary history of the buoyancy area and the mean compliance, respectively, for the case 2.

Table 1: Objective data for the cases from Fig. 5.

	Case 1	Case 2	Case 3
V_s	30%	30%	30%
B	0.1661 m ²	0.1575 m ²	0.1856 m ²
Compliance	$4.3030 \cdot 10^{-4}$ Nm	$3.7635 \cdot 10^{-4}$ Nm	$5.7643 \cdot 10^{-4}$ Nm

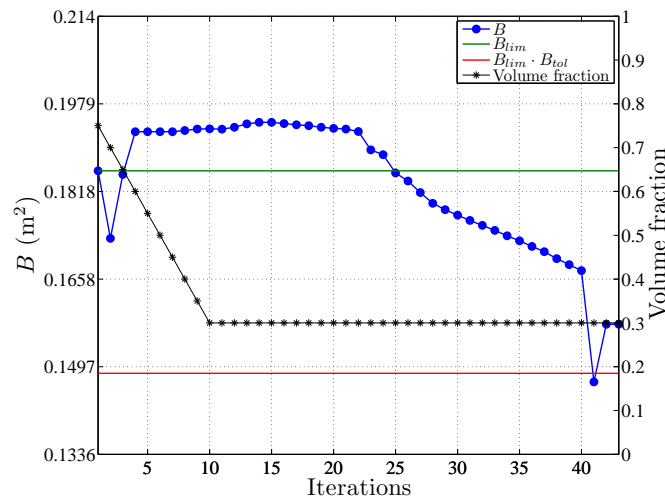


Figure 6: Evolutionary history of the buoyancy area for the case 2.

Figure 8 presents the strain energy distribution of the final structure in comparison with the case in which the boundaries are kept fixed. It can be observed that for the bubble-like

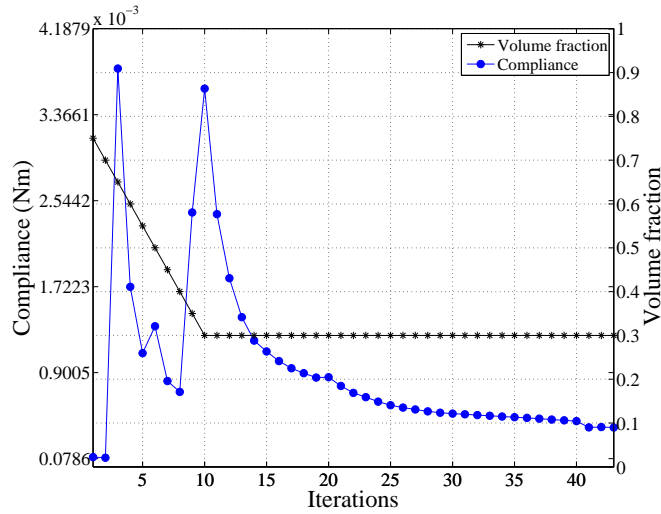


Figure 7: Evolutionary history of the buoy module's mean compliance for the case 2.

structure the strain energy distribution is much smoother than for the comparison case. Also, this result is reflected in the mean compliance value, which is around 35% smaller for the bubble-like buoy design. One important point to mention is that the proposed buoy module can be used in a fluid region where the drag forces are negligible, i.e., where the loads due to the subsea fluid flow are much smaller than the deep water pressure loads. If drag forces are considered further analysis should be carried out.

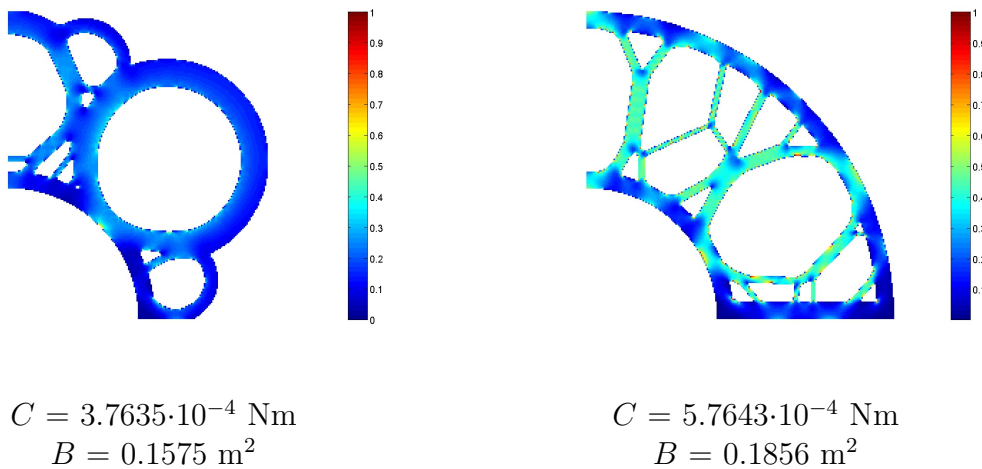


Figure 8: Strain energy distribution for the buoyancy module design with the proposed methodology and the case where the boundaries are kept fixed.

4 CONCLUSIONS

- A new methodology is proposed to seek alternative structural designs in offshore engineering, specifically in buoyant structures design.
- Design-dependent pressure loadings are handled straightforward with the evolutionary optimization methods.
- Comparing results with a case where the pressure loads are fixed, a stiffer structure can be designed moving the fluid-structure interfaces and fulfilling some buoyancy requirements simultaneously.
- The final topologies showed to be bubble-like structures, which strengthens the proposed methodology.
- If drag forces are negligible, the proposed solutions can inspire new buoyancy modules to be used in deep water conditions for support of oil pipelines.

REFERENCES

- [1] M.P. Bendsoe and N. Kikuchi. Generating optimal topologies in structural design using a homogenization method. *Comput. Methods. Appl. Mech. Engrg.* (1988) **71**:197–224.
- [2] G.H. Yoon, J.S. Jensen and O. Sigmund. Topology optimization of acoustic-structure interaction problems using a mixed finite element formulation. *Int. J. Numer. Methods Engrg.* (2007) **70**:1049–1075.
- [3] S. Kreissl, G. Pingen, A. Evgrafov and K. Maute. Topology optimization of flexible micro-fluidic devices. *Struct. Multidisc. Optim.* (2010) **42**:495–516.
- [4] O. Sigmund. and P.M. Clausen. Topology optimization using a mixed formulation: An alternative way to solve pressure load problems. *Comput. Methods. Appl. Mech. Engrg.* (2007) **196**:1874–1889.
- [5] E. Lee and J.R.R.A. Martins. Structural topology optimization with design-dependent pressure loads. *Comput. Methods. Appl. Mech. Engrg.* (2012) **233–236**:40–48.
- [6] Y.M. Xie and X. Huang. *Evolutionary Topology Optimization of Continuum Structures: Methods and Applications*. West Sussex: John Wiley and Sons, Ltd. 1st ed., (2010).
- [7] Zienkiewicz, O.C. and Taylor, R.L. *The finite element method*. McGraw Hill, Vol. I., (1989), Vol. II., (1991).